VIBRATIONAL ANALYSIS OF THE ALL-*TRANS* RETINAL PROTONATED SCHIFF BASE

STEVEN O. SMITH,* ANNE B. MYERS,* RICHARD A. MATHIES,* JOHANNES A. PARDOEN,‡ CHRIS WINKEL,‡ ELLEN M. M. VAN DEN BERG,‡ AND JOHAN LUGTENBURG‡
*Department of *Chemistry, University of California, Berkeley, California 94720; and Department of ‡Chemistry, Leiden University, 2300 RA Leiden, The Netherlands*

ABSTRACT We have obtained Raman spectra of a series of all-*trans* retinal protonated Schiff-base isotopic derivatives. ^{13}C-substitutions were made at the 5, 6, 7, 8, 9, 10, 11, 12, 13, 14, and 15 positions while deuteration was performed at position 15. Based on the isotopic shifts, the observed C—C stretching vibrations in the 1,100–1,400 cm^{-1} fingerprint region are assigned. Normal mode calculations using a modified Urey-Bradley force field have been refined to reproduce the observed frequencies and isotopic shifts. Comparison with fingerprint assignments of all-*trans* retinal and its unprotonated Schiff base shows that the major effect of Schiff-base formation is a shift of the C_{14}—C_{15} stretch from 1,111 cm^{-1} in the aldehyde to ~1,163 cm^{-1} in the Schiff base. This shift is attributed to the increased C_{14}—C_{15} bond order that results from the reduced electronegativity of the Schiff-base nitrogen compared with the aldehyde oxygen. Protonation of the Schiff base increases π-electron delocalization, causing a 6 to 16 cm^{-1} frequency increase of the normal modes involving the C_8—C_9, C_{10}—C_{11}, C_{12}—C_{13}, and C_{14}—C_{15} stretches. Comparison of the protonated Schiff base Raman spectrum with that of light-adapted bacteriorhodopsin (BR_{568}) shows that incorporation of the all-*trans* protonated Schiff base into bacterio-opsin produces an additional ~10 cm^{-1} increase of each C—C stretching frequency as a result of protein-induced π-electron delocalization. Importantly, the frequency ordering and spacing of the C—C stretches in BR_{568} is the same as that found in the protonated Schiff base.

INTRODUCTION

The Schiff bases of retinal serve as the light-sensitive prosthetic groups in both rhodopsin, the vertebrate visual pigment, and bacteriorhodopsin, the light-driven proton pump of *Halobacterium halobium* (1, 2). The retinal chromophore in rhodopsin is an 11-*cis* protonated Schiff base (PSB) that photoisomerizes to a distorted all-*trans* configuration in the formation of the primary photoproduct, bathorhodopsin (3). Thermal decay of bathorhodopsin produces distinct spectral intermediates containing both protonated and unprotonated all-*trans* Schiff bases. In contrast to rhodopsin, the retinal chromophore in light-adapted bacteriorhodopsin (BR_{568}) is an all-*trans* protonated Schiff base that undergoes a cyclic photochemical reaction involving both chromophore isomerization about the C_{13}=C_{14} bond and Schiff base deprotonation/reprotonation. Thus, the protonated Schiff base of all-*trans* retinal plays an important role in the photochemistry of both pigments.

Raman and infrared vibrational spectra have been obtained of the retinal chromophore in both rhodopsin and bacteriorhodopsin in an effort to determine the molecular mechanism of excitation in these systems (4–7). Comparison of pigment spectra with those of retinal Schiff base model compounds has been used qualitatively to examine the chromophore configuration in rhodopsin (8) and its photointermediates (3, 9–11), and in bacteriorhodopsin (12–15). However, since the protein environment can alter both the frequencies and intensities of the vibrational lines, accurate interpretation of these pigment spectra requires specific vibrational assignments in the pigments and in the retinal model compounds. Early assignments of all-*trans* retinal were made by Rimai et al. (16) and Cookingham et al. (17). Recently, a more detailed assignment and analysis of the retinal isomers has been carried out by Curry et al. (18–20), and calculations have also been reported by Saito and Tasumi (21). However, the vibrational spectra of the Schiff bases and protonated Schiff bases of retinal have not yet been analyzed.

Here we present Raman spectra of the protonated Schiff base of all-*trans* retinal (*I*)

SCHEME I

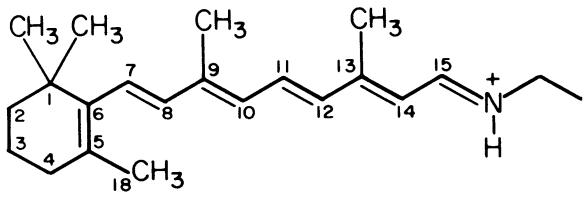

I

and its ^{13}C-isotopic derivatives. These isotopic derivatives were selected to assign the major C—C stretching vibrations in the 1,100–1,400 cm^{-1} fingerprint region. By comparing the protonated Schiff-base spectrum and assignments with those of the retinal aldehyde and Schiff base, the effects of Schiff-base formation and protonation of the Schiff-base nitrogen are elucidated. Further comparison with spectra of BR_{568} allows us to identify and interpret the spectral changes that result from incorporation of the retinal protonated Schiff base into bacterioopsin.

MATERIALS AND METHODS

Experimental Methods

All-*trans* retinal derivatives were synthesized according to recently published procedures (22–24). The ^{13}C-derivatives were 92% isotopically pure at each position and ≥98% isomerically pure as shown by mass spectrometry, nuclear magnetic resonance (NMR) spectroscopy, and high-performance liquid chromatography. The C_{15}—D derivative was ≥98% isotopically and isomerically pure. Crystalline all-*trans* retinal was purchased from Eastman Kodak Co. (Rochester, NY) and used without further purification.

The Schiff base of all-*trans* retinal was synthesized by addition of *n*-butylamine (threefold excess) to ~1 mg of retinal in 1 ml of dry diethyl ether at 0°C. The reaction was carried out over 4-Å molecular sieves in a thin-walled centrifuge tube. After 30 min, the ether and excess *n*-butylamine were evaporated with dry nitrogen, and the unprotonated Schiff base was redissolved in ether. Protonation was accomplished by addition of ether saturated with HCl gas. Crystals of the protonated Schiff base were pelleted and washed once with ether. The excess ether was evaporated with dry nitrogen and the tube sealed under nitrogen to prevent oxidation during the Raman experiments.

Raman spectra of the protonated Schiff base (PSB) were obtained using 25–30 mW of 752-nm excitation (cylindrically focused) from a Spectra Physics 171-01 krypton ion laser (Spectra-Physics Inc., Mountain View, CA). Raman spectra of the unprotonated Schiff base in CCl_4 were obtained using 40 mW of 676-nm excitation cylindrically focused on a stationary sample. In both cases, the far-red laser excitation was used to minimize photoisomerization of the sample. No evidence of isomerization or sample degradation was observed in successive scans. The data were smoothed using a three-point sliding average. The spectral resolution was 4 cm^{-1} and peak positions are accurate to 2 cm^{-1}.

Computational Methods

Vibrational calculations were performed using the Wilson FG method as described by Curry et al. (18). The geometry of the all-*trans* retinal protonated Schiff base was calculated using the QCFF/PI method (25). The *n*-butyl group was replaced by a CH_2R group, where R is an atom having mass 15, unit valence, and the potential parameters of a saturated carbon atom. The sp^3 carbon centers were forced to be tetrahedral and carbons 1, 4, and 18 of the ionone ring were replaced by R atoms. The initial force field for atoms distant from the Schiff base was the same as the most recent version used for all-*trans* retinal (20); force constants for the HC=NH—CH_2R group were set equal to the values used for the most nearly equivalent groups of all-*trans* retinal (Table I). The HC=N and C=NH Urey-Bradley constants were adjusted to fit the shifts of the 1,654 cm^{-1} C=N stretching mode in the 15-deuterio (15D) and N-deuterio (ND) derivatives. The force constants for the conjugated chain stretches from C_8 to N, as well as the HC=N and C=NH bending constants, were then refined to fit the observed frequencies (or, when appropriate, frequency shifts) of the PSB derivatives. The essential assumption is that the remaining constants are best constrained to reliable values derived from smaller model compounds and all-*trans* retinal where more extensive isotopic data were employed in the analysis. Thus, the bending Urey-Bradley and non–Urey-Bradley constants for interactions distinct from the Schiff base and for the methyl groups were unchanged from the retinal values. At least for the CCH rocks, all of which have the same constants, this is justified. The vinyl rocks at 1,270 and 1,280 cm^{-1} are at virtually the same frequency in the aldehyde, the Schiff base, and the protonated Schiff base (see below). Ten force constants (see Table I) were adjusted to fit 128 in-plane frequencies of the unsubstituted, 15D, and ^{13}C-labeled derivatives with a rms error of 5.3 cm^{-1} (maximum error 15 cm^{-1}).

RESULTS

C—C Stretches

The 1,100–1,400 cm^{-1} fingerprint region consists of mixed C—C stretching and CCH rocking vibrations whose frequencies and intensities are sensitive to the geometry of the retinal chromophore. The contribution of a particular C—C internal coordinate to a fingerprint normal mode can be accurately determined from its ^{13}C-shift. Thus, it is convenient to discuss the fingerprint vibrations in terms of their C—C stretch character, which is in many cases highly localized, even though each mode has significant contributions from CCH rocks. For example, the spectra in Fig. 1 show that a normal mode consisting predominantly of the C_{14}—C_{15} stretch is localized at 1,191 cm^{-1} in the native PSB spectrum. This is based on the 19 cm^{-1} shift of this line to 1,172 cm^{-1} in the 14,15-di[^{13}C] derivative. The C_{14}—C_{15} coordinate contributes only slightly to one other fingerprint mode at 1,237 cm^{-1} in the native spectrum as evidenced by the 3 cm^{-1} shift of this line in the 14,15-di[^{13}C] derivative. Similarly, the 1,159 cm^{-1} line in the native spectrum is clearly assigned as the C_{10}—C_{11} stretch based on its 12 cm^{-1} shift to 1,147 cm^{-1} in the 10,11-di[^{13}C] spectrum (Fig. 1 *E*). The C_{10}—C_{11} stretching coordinate in this derivative mixes with and donates intensity to modes at 1,114 and 1,121 cm^{-1}, which can be assigned to ionone ring modes based on their correspondence to the 1,123 and 1,134 cm^{-1} ionone ring modes in all-*trans* retinal (18). The C_8—C_9 stretch is assigned to the 1,204 cm^{-1} line in the native PSB spectrum based on an ~9 cm^{-1} shift of this line to ~1,195 cm^{-1} upon ^{13}C-substitution at C_9 (Fig. 1 *F*). Labeling at C_{13} (Fig. 1 *C*) results in a shift in both the 1,159 cm^{-1} line (3 cm^{-1}) and the 1,237 cm^{-1} line (7 cm^{-1}). The normal mode having the most C_{12}—C_{13} character is the 1,237 cm^{-1} line although this internal coordinate is not highly localized in any one normal mode. Interestingly, neither 8-[^{13}C] nor 12-[^{13}C] substitution causes significant shifts of the 1,204 or 1,237 cm^{-1} lines, respectively. As will be discussed below this is a unique characteristic of methyl-substituted C—C stretches. Finally, the C_6—C_7 stretch is apparently too weak or delocalized to be observed; no significant vibrational shifts occur in the fingerprint region of the 6-[^{13}C] and 7-[^{13}C] PSB derivatives (Figs. 1 *H* and *I*). However, the C_6—C_7

TABLE I

ALL-*TRANS* RETINAL PROTONATED SCHIFF-BASE FORCE FIELD*

Coordinate	Force constant
Chain stretches	
K(5═6)	6.40
K(7═8)	6.56
K(9═10)‖	6.34 (6.22)
K(11═12)‖	6.22 (6.46)
K(13═14)‖	6.20 (6.10)
K(6—7)	3.57
K(8—9)‖	3.48 (3.6)
K(10—11)‖	3.86 (3.85)
K(12—13)‖	4.13 (3.63)
K(14—15)‖	4.01 (3.13)
K(C—R)	3.07
K(C—H)	4.827
K($C_{15}H$)	4.00
Chain bends	
H(CCC)	0.570
H(C═CH)	0.288
H(C—CH)	0.300
H(CCC) R group	0.75
H(CCC) cis‡	0.82
Urey-Bradley	
F(C═ CH)	0.52
F(C—CH)	0.49
F(CC—CH_3)	0.59
F(CCC)	0.35
Non–Urey-Bradley	
k(C═C, C═C) one bond apart	−0.31
k(5═6, 7═8)	−0.02
k(C═C, C—C) adjacent	0.056
k(C—C, C—C) one bond apart	−0.09
k(CC, C—CH_3) adjacent	−0.14
k(CC, CC) long range§	−0.04
m(CC, bend)	0.07
h(CCH, CCH) or h(CCC, CCH) *trans*	0.06
h(CCC, CC—CH_3) *trans*	0.04
h(CCC, CC—CH_3) *cis*	0.338
h(CCC, CCC) *trans*	0.145
h(CCC, CCC) *cis*	0.17
CH_3 group	
K(CH)	4.709
H(CCH)	0.389
H(HCH)	0.506
F(CCH)	0.48
h(HCH, HCH)	−0.012
h(CCH, CCH)	0.034
K(C—CH_3)	2.55
F(HCH)	0.13
New coordinates	
K(C═N)‖	7.85
K(N—C)	2.75
K(NH)	4.83
K(CH) *n*-butyl	4.71
K(CR) *n*-butyl	2.23
H(C—C═N)	0.57
H(HC═N)‖	0.272
H(C═NH)‖	0.392
H(C═N—C)	0.82
H(HN—C)	0.329
H(N—CH)	0.389
H(N—C—R)	0.69
H(HCH) *n*-butyl	0.506
H(R—CH)	0.329
F(C—C═N)	0.80
F(HC═N)	0.80
F(C═NH)	0.30
F(C═N—C)	0.59
F(HN—C)	0.55
F(N—CH)	0.48
F(N—C—R)	0.32
F(HCH) *n*-butyl	0.13
F(R—CH)	0.55
h(HC═N, C═NH)	0.05

*Modified Urey-Bradley force field adapted from reference 20. The symbol ‖ indicates force constants that were adjusted during refinement. Numbers in parentheses are initial all-*trans* retinal force constants. Symbols used: K, diagonal stretch; H, diagonal bend; F, Urey-Bradley quadratic constant (linear term set equal to −0.1 F); k, stretch-stretch interaction; h, bend-bend interaction (two common atoms); m, stretch-bend interaction (one common atom). Stretching force constants in millidynes per angstrom, stretch-bend cross terms in millidynes per radian, bending constants in millidynes per angstrom per radian squared. A listing of the geometry can be obtained by writing the authors.

‡Applies to all CCC or $CCCH_3$ bends that are *cis* to another such bend.

§Applies to pairs of chain stretches separated by three or five bonds. Interactions involving the C_5═C_6 bond have not been included.

stretch should appear at a similar frequency to that found in all-*trans* retinal (1,174 cm^{-1}).

The calculated normal modes for the all-*trans* PSB are given in Table II, and the calculated and observed ^{13}C-shifts are summarized in Table III. It is important to realize that the contribution of a C—C internal coordinate to the potential energy of a normal mode is $\sim\sqrt{6}$ larger than a CCH rock with a similar coefficient because of their different reduced mass. Therefore, despite the significant contribution of CCH rocks to the modes in the 1,150–1,250

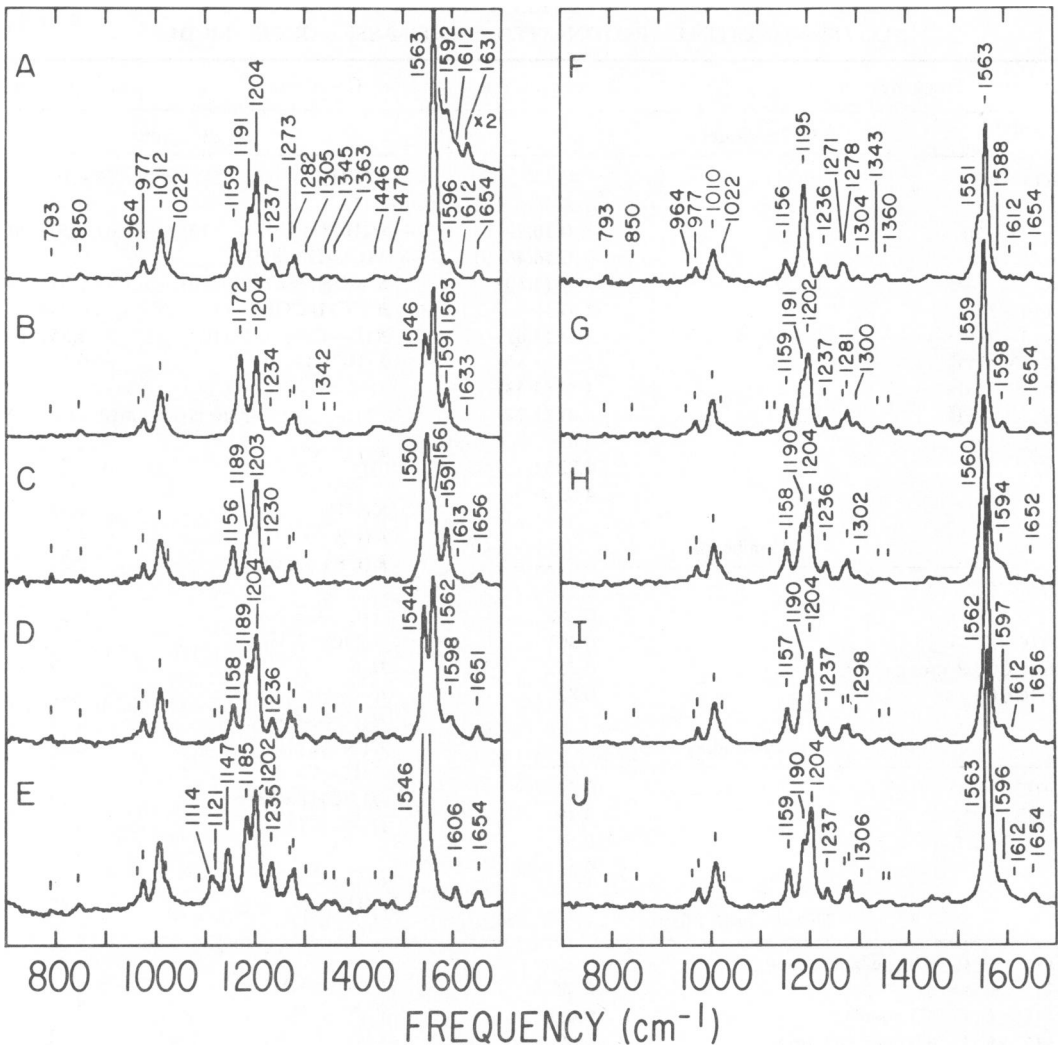

FIGURE 1 Raman spectra of the protonated *n*-butylamine Schiff base of all-*trans* retinal (*A*), and its 14,15-di[^{13}C] (*B*), 13-^{13}C (*C*), 12-^{13}C (*D*), 10,11-di[^{13}C] (*E*), 9-^{13}C (*F*), 8-^{13}C (*G*), 7-^{13}C (*H*), 6-^{13}C (*I*) and 5-^{13}C (*J*) derivatives. Spectra were obtained from microcrystalline precipitates of the chloride salt at room temperature with 752-nm excitation. The insert in *A* gives the spectrum of the Schiff-base region for the ND derivative.

cm^{-1} region, these modes are best discussed as C—C stretches. The C_{14}—C_{15} stretch is calculated at 1,187 cm^{-1} and is relatively localized, with a small out-of-phase contribution from the C_{12}—C_{13} stretch. The C_8—C_9 stretch is calculated at 1,199 cm^{-1} as a symmetric combination of the C_8—C_9, C_{10}—C_{11}, and C_{14}—C_{15} stretches, consistent with its large Raman intensity.[1] The good agreement between the calculated and observed ^{13}C-shifts (Table III) for the 1,204 cm^{-1} C_8—C_9 stretch demonstrates that the normal mode description is qualitatively correct. The C_{12}—C_{13} stretch is calculated at 1,223 cm^{-1} and contains a large contribution from the C_{14}—C_{15} stretch and the $C_{14}H$ rock. We were not able to accurately reproduce the experimental 1,237 cm^{-1} frequency of the C_{12}—C_{13} stretching vibration or to obtain enough C_{12}—C_{13} stretch character in the 1,159 cm^{-1} mode to be responsible for the 3 cm^{-1} shift of this line in the 13-[^{13}C] derivative (Table III). The calculated normal mode at 1,223 cm^{-1} is 14 cm^{-1} lower than observed, even with a C_{12}—C_{13} stretching force constant that is considerably elevated over that of all-*trans* retinal. Further increases in the C_{12}—C_{13} force constant act mainly to drive stretching character out of the 1,223

[1]The intensity of a normal mode in the Raman spectrum is a function of the magnitude of the coefficients of each of the internal coordinates that make up the mode as well as the individual bond length changes that occur in each internal coordinate upon electronic excitation. In addition the intensity will depend on the phase with which these internal coordinates are combined to form the normal mode. For example, in a normal mode that is a symmetric combination of more than one C—C stretch, the individual bond length changes will contribute constructively to give an intense Raman line. In an antisymmetric combination, cancellation will occur and the Raman intensity will be reduced. This is generally true for polyenes because the C—C bond lengths all decrease in the excited state. Parallel arguments apply for the double-bond stretches.

TABLE II
ALL-*TRANS* RETINAL PROTONATED SCHIFF-BASE NORMAL MODES

Frequency		Normal mode
Experimental	Calculated	
1,654 cm^{-1}	1,654 cm^{-1}	0.35(C=N) − 0.18(14—15) + 0.61(15H) − 0.67(NH)
—	1,609	0.40(5=6) − 0.16(6—7)
1,612	1,597	0.30(7=8) − 0.18(9=10) − 0.11(11=12) − 0.13(6—7) + 0.14(10—11) − 0.08(8—9) + 0.54(7H) − 0.40(8H)
1,596	1,589	0.33(13=14) − 0.14(7=8) − 0.13(9=10) − 0.13(14—15) − 0.49(14H)
1,563	1,568	0.31(9=10) + 0.15(13=14) − 0.15(11=12) − 0.12(8—9) + 0.07(12—13)
	1,563	0.31(11=12) − 0.18(12—13) − 0.15(10—11) − 0.59(12H) + 0.56(11H)
1,363	1,365	0.56(14H) − 0.51(15H) − 0.24(13—CH_3) + 0.11(12—13) + 0.13(14—15)
~1,350	1,356	0.67(NH) − 0.59(10H) + 0.15(9—CH_3) + 0.17(12—13)
	1,348	0.77(NH) − 0.52(15H)
1,345	1,338	0.62(15H) + 0.53(10H) + 0.45(NH) + 0.12(8—9) + 0.12(12—13) − 0.16(9—CH_3)
1,305	1,307	0.65(8H) + 0.45(12H) − 0.29(15H) + 0.23(8—9) − 0.11(6—7) − 0.11(9—CH_3)
1,282	1,287	0.94(7H) − 0.43(12H) − 0.11(7=8)
	1,284	0.62(12H) − 0.61(8H) + 0.12(11=12)
1,273	1,274	0.94(11H) − 0.56(8H) + 0.10(12—13)
1,237	1,223	0.12(12—13) + 0.08(14—15) − 0.83(14H) − 0.04(13—CH_3) + 0.03(11=12) − 0.04 (13=14) − 0.34(12H)
1,204	1,199	0.15(8—9) + 0.07(14—15) + 0.08(10—11) − 0.74(10H) − 0.07(9—CH_3) − 0.04(9=10) − 0.05(11=12)
1,191	1,187	0.26(14—15) − 0.11(12—13) − 0.34(12H) − 0.35(15H) − 0.27(11H)
—	1,178	0.23(6—7) + 0.40(7H)
1,159	1,162	0.27(10—11) − 0.12(8—9) + 0.32(11H) − 0.03(14—15)
1,131	—	β-ionone ring mode
1,121	—	β-ionone ring mode
1,022	1,019	0.63($9CH_3r$) − 0.28($13CH_3r$) − 0.05(8—9)
1,012	1,009	0.72($13CH_3r$) + 0.21($9CH_3r$) − 0.06(12—13)
977 / 964	—	11,12—A_u HOOP and 7,8—A_u HOOP
—	865	0.15(9—CH_3) + 0.06(8—9) + 0.19(13—CH_3) + 0.05(12—13)
—	841	0.18(9—CH_3) + 0.07(8—9) − 0.15(13—CH_3) − 0.06(12—13)
793	—	β-ionone ring mode

Coefficients ($\partial S/\partial Q$) of internal coordinates S in the normal modes Q. Symbols used: H, in-plane hydrogen rock; r, methyl rock; HOOP, hydrogen out-of-plane wag.

cm^{-1} mode without significantly raising its frequency. Because of the large contribution of the $C_{14}H$ rocking coordinate to this normal mode, its frequency is sensitive to the CCH rocking force constant and to the interaction constant between the C_{12}—C_{13} stretch and the $C_{14}H$ rock. Deuterated derivatives of the PSB should be examined to accurately refine these constants. Nevertheless, the good agreement between the calculated and observed shifts of the 1,237 cm^{-1} line in the 13-[^{13}C] and 14,15-di[^{13}C] derivatives (Table III) indicates that at least the calculated C—C character in this normal mode is reasonably correct.

Effect of Methyl Groups on the C_8—C_9 and C_{12}—C_{13} Stretches

The distinctive pattern of vibrational frequencies and intensities in the fingerprint region of retinal compounds results in part from the presence of the C_9- and C_{13}-methyl groups on the polyene chain. Kinetic coupling of the C_8—C_9 and C_{12}—C_{13} stretches with the C_9—CH_3 and C_{13}—CH_3 stretches, respectively, results in symmetric and antisymmetric combinations of these internal coordinates in the normal modes. The symmetric combinations, C_8—C_9 + C_9—CH_3 and C_{12}—C_{13} + C_{13}—CH_3, are calculated between 840 and 870 cm^{-1} with no significant contributions from other internal coordinates (see Table II). However, the antisymmetric combinations of these stretches are higher in frequency than the other unsubstituted C—C stretches, and they interact strongly with the CCH in-plane rocks and C=C stretches. In the case of all-*trans* and 13-*cis* retinal, the antisymmetric stretch combinations were calculated and observed to couple strongly with the $C_{10}H$ and $C_{14}H$ rocks (18–20). Similarly, in the PSB the C_8—C_9 − C_9—CH_3 combination is calcu-

TABLE III
^{13}C-SHIFTS FOR C—C STRETCHING VIBRATIONS*

Derivative	Principal C—C stretch component			
	C_8—C_9	C_{10}—C_{11}	C_{12}—C_{13}	C_{14}—C_{15}
Native	1,204 (1,199)	1,159 (1,162)	1,237 (1,223)	1,191 (1,187)
14,15-di[^{13}C]	0 (1)	§ (5)	3 (3)	19 (23)
13-[^{13}C]	1 (0)	3 (0)	7 (6)	2 (5)
12-[^{13}C]	0 (0)	1 (0)	1 (2)	2 (2)
10,11-di[^{13}C]	2 (3)	12 (28)‡	2 (1)	6 (0)
9-[^{13}C]	9 (7)	3 (5)	1 (1)	§ (0)
8-[^{13}C]	2 (2)	0 (1)	0 (0)	0 (0)

*Calculated ^{13}C-shifts are in parentheses. All frequencies are in wavenumbers.
‡The calculated shift for the 10,11-di[^{13}C] derivative is larger than that observed because the downshifted C_{10}—C_{11} stretch couples with β-ionone ring modes at 1,121 and 1,131 cm^{-1}. The sum of the ^{13}C-shifts of the ionone lines (17 cm^{-1}) and the C_{10}—C_{11} stretch (12 cm^{-1}) is close to the calculated shift of 28 cm^{-1}.
§Not resolved.

lated to contribute to normal modes at 1,199, 1,307, and 1,338 cm^{-1}. Of these three modes, significant $C_{10}H$ rock character is calculated at 1,199 and 1,338 cm^{-1}. The C_{12}—C_{13} – C_{13}—CH_3 combination is calculated to contribute to normal modes at 1,223 and 1,365 cm^{-1}, both of which contain significant $C_{14}H$ rock character.

The calculated normal modes for the C_{12}—C_{13} stretch, the C_8—C_9 stretch, and the C_{10}—C_{11} stretch are depicted in Fig. 2 *A, B,* and *C,* respectively. It is apparent from the atomic displacements that the methyl substituted carbons (13 and 9) move considerably more than carbons 12 and 8 in the C_{12}—C_{13} and C_8—C_9 stretching modes, respectively. These modes are highly mixed combinations of the C—C, C=C, and C—CH_3 stretches and CCH in-plane rocks, whereas the 1,162 cm^{-1} mode (Fig. 2 *C*) is better described as a localized C_{10}—C_{11} stretch. It is the reduction of C—C stretch character in the 1,223 and 1,199 cm^{-1} modes, in addition to increased CCH rock and C=C stretch character, which accounts for the reduced motion of C_8 and C_{12} in these modes and hence the reduced sensitivity to ^{13}C-substitution at these positions.

To determine the origin of the different isotopic shifts observed between the C_8 and C_9, or C_{12} and C_{13} positions, it is useful to separate the net displacement of each atom into the Cartesian displacements contributed by each internal coordinate. We begin by examining the 1,223 cm^{-1} C_{12}—C_{13} stretch. Since the magnitude of the displacements along the *y*-axis are nearly the same for C_{12} and C_{13} (see Fig. 2 *A*), we need only examine the displacements in the *x* direction in detail. The displacement of C_{12} along the *x*-axis due to the C_{12}—C_{13} stretch is calculated as −0.052 Å. This motion is almost exactly canceled by the *x* displacements of C_{12} due to the C_{11}=C_{12} stretch (+0.021 Å) and the $C_{12}H$ rock (+0.032 Å). However, for C_{13} the *x* displacement due to the C_{12}—C_{13} stretch (+0.052 Å) adds to that calculated for the C_{13}=C_{14} stretch (+0.033 Å).

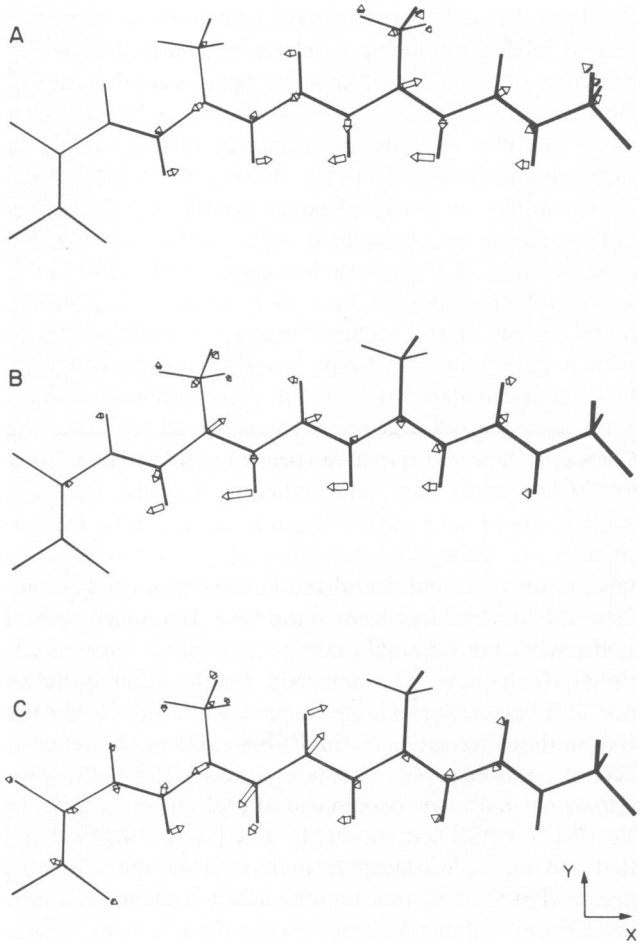

FIGURE 2 Mass-weighted atomic displacements for selected in-plane normal modes of the all-*trans* retinal PSB. (*A*) The C_{12}—C_{13} stretch (1,223 cm^{-1}). (*B*) The C_8—C_9 stretch (1,199 cm^{-1}). (*C*) The C_{10}—C_{11} stretch (1,162 cm^{-1}).

The other internal coordinates contribute very little to the motion of C_{12} or C_{13} along the x-axis, so that the net motion in the x direction is much greater for C_{13} (+0.088 Å) than for C_{12} (~0.0 Å). It is these differences in the magnitude of x displacement, primarily due to the phase with which the C_{11}=C_{12} and C_{13}=C_{14} stretches mix with the C_{12}—C_{13} stretch, that lead to the large motion at C_{13} compared with C_{12} and hence the observed differences in sensitivity to ^{13}C-labeling. This contribution of the double-bond internal coordinates to the C—C stretches can also help to explain the difference in intensity between the C_8—C_9 and the C_{12}—C_{13} stretching modes. The weak intensity of the 1,237 cm^{-1} line may result from the C_{13}=C_{14} and C_{11}=C_{12} stretches that contribute out-of-phase with nearly equal coefficients (Table II).

C=C Stretches

Assignment of the ethylenic modes is more difficult because the intrinsic frequencies of the C=C stretches are closer together and thus they mix much more with each other in the normal modes. The intense ethylenic band at 1,563 cm^{-1} is calculated to have contributions from two normal modes, one being a relatively localized C_{11}=C_{12} stretch at 1,563 cm^{-1} and the other being a combination of the C_9=C_{10}, C_{11}=C_{12}, and C_{13}=C_{14} stretches at 1,568 cm^{-1}. We can evaluate the accuracy of the calculated mode character by selectively shifting the various local C=C components down in frequency with ^{13}C-substitution and comparing with calculated shifts. In the 13-[^{13}C] PSB spectrum (Fig. 1 *C*), a new line appears at 1,550 cm^{-1}, presumably resulting from a shift of C_{13}=C_{14} stretch character out of the higher frequency normal modes to form a new, more localized, lower frequency vibration. This line is calculated at 1,552 cm^{-1} and contains substantially more C_{13}=C_{14} stretch character (0.30) than the 1,568 cm^{-1} line in the native spectrum (0.15). The intensity of the 1,550 cm^{-1} line indicates that the C_{13}=C_{14} internal coordinate carries significant intrinsic Raman intensity. In the 9-[^{13}C] derivative (Fig. 1 *F*), a new line appears at 1,551 cm^{-1} and the calculations predict that C_9=C_{10} character increases in the lower frequency normal mode, while the C_{13}=C_{14} component moves up into the higher frequency antisymmetric combination (~1,588 cm^{-1}). The relatively high frequency of the ^{13}C-shifted lines in these derivatives is consistent with the existence of C_9=C_{10} and C_{13}=C_{14} character in only the higher frequency normal mode component of the ethylenic band. In the 12-[^{13}C] PSB spectrum (Fig. 1 *D*), a new line appears at 1,544 cm^{-1}, resulting from a shift of the C_{11}=C_{12} stretch. The C_{11}=C_{12} stretching mode is calculated to shift to 1,538 cm^{-1} in this derivative, while the 1,568 cm^{-1} mode is now a combination of mainly the C_9=C_{10}, C_{13}=C_{14}, and C_7=C_8 stretches with no change in frequency. The low frequency of the 1,544 cm^{-1} line in this mono-^{13}C-derivative is consistent with the description of the lower frequency mode in the native spectrum as predominantly the C_{11}=C_{12} stretch. The shifted 1,544 cm^{-1} line carries nearly half of the overall ethylenic intensity. In the 10,11-di[^{13}C] PSB spectrum (Fig. 1 *E*) both the C_9=C_{10} and C_{11}=C_{12} components of the 1,563 cm^{-1} band are shifted resulting in only one intense line at 1,546 cm^{-1}. This dramatically demonstrates that the majority of the ethylenic Raman intensity arises from the C_9=C_{10} and C_{11}=C_{12} double-bond stretches. The calculation reproduced these shifts yielding a C_9=C_{10} + C_{11}=C_{12} combination at 1,541 cm^{-1} and a C_9=C_{10} − C_{11}=C_{12} combination at 1,549 cm^{-1}. C_{13}=C_{14} character is calculated to shift up into the higher frequency mode at 1,589 cm^{-1} in the 10,11-di[^{13}C] PSB, where it presumably mixes out-of-phase with other internal coordinates, canceling its intensity. The reasonable reproduction of the ^{13}C-shifts provides evidence that the normal mode description of the 1,563 and 1,568 cm^{-1} modes in Table II is qualitatively correct. A more accurate determination of these C=C normal modes awaits a detailed analysis of the Raman intensity as well as deuterium derivative data.

The C_5=C_6 and C_7=C_8 stretches are calculated at 1,609 and 1,597 cm^{-1}, respectively. The C_5=C_6 stretch cannot be assigned since no frequency or intensity changes are observed in the 5-[^{13}C] or 6-[^{13}C] PSB spectra (Figs. 1 *I, J*). The C_7=C_8 stretch is also difficult to assign. The calculated normal mode for the C_7=C_8 stretch is an antisymmetric combination of the C_7=C_8 stretch with the C_9=C_{10} and C_{11}=C_{12} stretches. The observed increase of intensity at 1,606 cm^{-1} in the 10,11-di[^{13}C] PSB spectrum (Fig. 1 *E*) suggests that this mode can be assigned to the C_7=C_8 stretch since the out-of-phase contributions from the C_9=C_{10} and C_{11}=C_{12} stretches, which cancel C_7=C_8 intensity in the native spectrum, will be reduced when these stretches are shifted to lower frequencies in the 10,11-di[^{13}C] derivative. The C_7=C_8 stretching mode is calculated to have shifted down 5 cm^{-1} in the 10,11-di[^{13}C] derivative. This suggests that the C_7=C_8 stretching mode in the native PSB spectrum is 5 cm^{-1} above its position in the 10,11-di[^{13}C] derivative. Thus, the weak shoulder at 1,612 cm^{-1} is assigned as the C_7=C_8 stretch in the native spectrum. This is in agreement with recently published all-*trans* retinal assignments based on ^{13}C-derivatives (20).

Finally, the remaining C=C stretching mode at 1,596 cm^{-1} contains contributions from both the C_9=C_{10} and C_{13}=C_{14} stretches. In the 13-[^{13}C] and 14,15-di[^{13}C] PSB derivatives, the 1,596 cm^{-1} line shifts 5 cm^{-1} to 1,591 cm^{-1}, while in the 9-[^{13}C] derivative this line has disappeared, possibly shifting 8 cm^{-1} to 1,588 cm^{-1}. These results are in reasonable agreement with the calculation that predicts an antisymmetric combination of the C_{13}=C_{14}, C_7=C_8, and C_9=C_{10} stretches at 1,589 cm^{-1}.

The C=N stretch can be assigned to the 1,654 cm^{-1} line based on its 21 cm^{-1} shift to 1,633 cm^{-1} in the 14,15-

di[^{13}C] derivative (Fig. 1 *B*), and a 14 cm^{-1} shift in the ^{15}N-PSB (shifts summarized in Table IV). Since an isolated C=N stretch would be expected to shift ~35 cm^{-1} upon ^{13}C-substitution at C_{15} or ^{15}N-substitution of the Schiff-base nitrogen, other internal coordinates must contribute to the normal mode. The insensitivity of the 1,654 cm^{-1} line to ^{13}C-substitution at other positions along the retinal chain shows that the chain C=C stretches do not contribute to this mode. For example, ^{13}C-substitution at C_{13} produces a large shift in the ethylenic modes that have C_{13}=C_{14} stretching character while no shift in the Schiff-base vibration is observed. Both the N—H and C_{15}—H in-plane rocks, however, are known to couple with the C=N stretch (11, 12). The extent of coupling is characterized by the ND- and 15D-induced shifts of the 1,654 cm^{-1} line (Table IV). In the ND PSB derivative, the 1,654 cm^{-1} line shifts 23 to 1,631 cm^{-1}, close to the 25–30 cm^{-1} shift observed in solution (14, 26), while 15-deuteration shifts the 1,654 cm^{-1} line 12 cm^{-1}.

Analysis of 15D Substitution

The 15D derivative of retinal has been used extensively in both Raman (12, 13, 27) and Fourier transform infrared spectroscopy (6, 7) studies on bacteriorhodopsin and rhodopsin. Analysis of the isotopic shifts observed in the 15D PSB spectrum should help to more clearly explain the changes observed in the pigment spectra. Raman spectra of 15D and 14,15-di[^{13}C],15D PSBs are shown in Fig. 3. The C_{15}—H in-plane rock is assigned at 1,345 cm^{-1} in the native PSB spectrum (1,338 cm^{-1} calculated) based on the disappearance of this line in the 15D PSB spectrum (Fig. 3 *A*); the deuterated rock is tentatively assigned at ~986 cm^{-1} (985 cm^{-1} calculated) based on the appearance of a shoulder at this frequency in the 15D and 14,15-di[^{13}C],15D spectra. Other changes in the fingerprint region of the 15D PSB spectrum result from removal of C_{15}—H rock coupling with the C—C single-bond stretches. In particular, the 1,191 and 1,237 cm^{-1} lines have either lost intensity or shifted in frequency, and the

TABLE IV
ISOTOPIC SHIFTS OF THE C=N STRETCHING MODE*

Derivative	PSB	BR_{568}‡
^{15}N	14§ (18)	13
14,15-di[^{13}C]	21 (30)	18
ND	23 (20)	16
15D	12 (12)	10

*Calculated shifts are in parentheses. All frequencies are in wavenumbers.

‡From Smith, S. O., M. S. Braiman, A. B. Myers, J. A. Pardoen, C. Winkel, P. P. J. Mulder, J. Lugtenburg, and R. Mathies. Manuscript in preparation.

§Spectrum not shown.

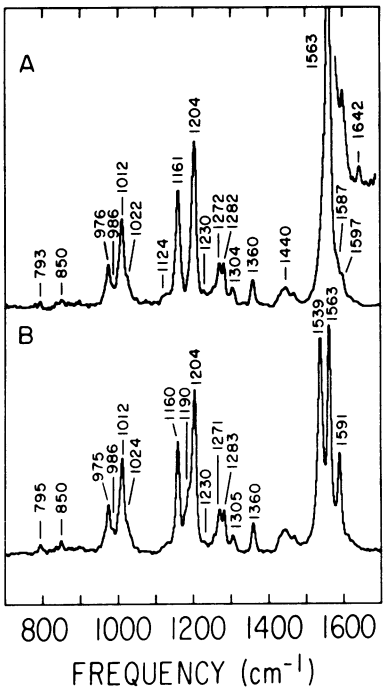

FIGURE 3 Raman spectra of the 15D all-*trans* retinal PSB (*A*) and the 14,15-di[^{13}C],15D derivative (*B*). The inset in *A* presents a high signal-to-noise spectrum of the Schiff-base region of the 15D PSB obtained with 15 mW of 676-nm excitation.

1,161 cm^{-1} line has gained intensity. Based on our calculations (Table V), the C_{14}—C_{15} stretch should shift up ~20 cm^{-1} upon 15-deuteration.[2] Thus, the C_{14}—C_{15} stretch at 1,191 cm^{-1} in the native PSB has probably shifted up beneath the intense 1,204 cm^{-1} line in the 15D derivative. The appearance of a shoulder at 1,190 cm^{-1} in the 14,15-di[^{13}C],15D derivative (Fig. 3 *B*) supports this conclusion since ^{13}C-substitution at positions 14 and 15 should shift the C_{14}—C_{15} stretch down by ~25 cm^{-1}, canceling the shift induced by 15-deuteration (Table VI). Increased intensity at 1,161 cm^{-1} in the 15D PSB presumably results from a decrease of C_{14}—C_{15} stretch character in this mode. Although the calculation shows only a small out-of-phase component of the C_{14}—C_{15} stretch at 1,162 cm^{-1} in the native PSB, this component is calculated to decrease in the 15D derivative. Loss of intensity in the 1,237 cm^{-1} C_{12}—C_{13} stretch upon 15-deuteration has been interpreted as being due to the shift of a normal mode involving mostly the C_{14}—C_{15} stretch and/or C_{15}—H rock (18, 27). However, the calculated 1,223 cm^{-1} line is a symmetric combination of the C_{12}—C_{13} and C_{14}—C_{15} stretches in the native PSB, which shifts down 1 cm^{-1} and becomes an isolated C_{12}—C_{13} stretch in the 15D derivative (Table V).[3] Thus,

[2]In all-*trans* retinal, a much larger shift (38 cm^{-1}) of the C_{14}—C_{15} stretch was observed upon 15-deuteration (18). The larger shift in all-*trans* retinal results from greater interaction with the C_{15}D rock, which is closer in frequency to the C_{14}—C_{15} stretch in all-*trans* retinal (1,111 cm^{-1}) than in the PSB (1,191 cm^{-1}).

TABLE V
15D PROTONATED SCHIFF-BASE C—C NORMAL MODES

Frequency		Normal mode
Experimental	Calculated	
cm^{-1}		
1,230	1,222	0.14(12—13) − 0.81(14H) − 0.41(12H) − 0.05(13—CH_3)
1,204	1,207	0.24(14—15) − 0.31(15D)
	1,198	0.14(8—9) − 0.72(10H) − 0.54(12H) − 0.33(8H) − 0.07(9—CH_3)
—	1,178	0.23(6—7) + 0.40(7H)
1,161	1,162	0.27(10—11) − 0.12(8—9) + 0.33(11H) − 0.01(14—15)

15-deuteration does not remove a normal mode from the 1,235 cm^{-1} region, but merely causes a change of intensity because of altered mixing with the C_{14}—C_{15} stretch. The weak lines at ~1,230 cm^{-1} in the 15D and 14,15-di[^{13}C],15D spectra may be due to the residual C_{12}—C_{13} stretch.

DISCUSSION

Now that the major fingerprint vibrations of both all-*trans* retinal (18) and the all-*trans* retinal PSB have been assigned, it is possible to compare the aldehyde, Schiff base and protonated Schiff-base spectra and discuss the effects of Schiff-base formation and protonation on the Raman spectrum. Furthermore, comparison of the PSB spectrum to that of BR_{568} should permit the identification of the spectral changes that result from protein binding. Fig. 4 presents Raman spectra of all-*trans* retinal, its unprotonated and protonated Schiff bases, and BR_{568}. The vibrational frequencies of the C—C stretches are correlated in Fig. 5.

We begin by summarizing the vibrational assignments of the C—C stretches in all-*trans* retinal (18). The lowest frequency stretch is the 1,111 cm^{-1} C_{14}—C_{15} stretch, which is an intense, easily assigned line in the infrared. The C_{10}—C_{11} stretch is at 1,163 cm^{-1}, a characteristic frequency for a single-bond stretch in an unsubstituted linear polyene. The two methyl-substituted stretches,

[3]Another possibility is that the 1,237 cm^{-1} line is actually an antisymmetric combination of the C_{12}—C_{13} and C_{14}—C_{15} stretches, and that 15-deuteration increases the contribution of the out-of-phase C_{14}—C_{15} stretch to this normal mode, which would reduce the Raman intensity. The calculated frequency ordering of the symmetric and antisymmetric stretch combinations can be changed most simply by adjusting the (C_{12}—C_{13}, C_{14}—C_{15}) coupling constant. The magnitude of this coupling constant must be increased from −0.09 to approximately −0.40 to put the antisymmetric combination above the symmetric one. Such a large change in the force field from the all-*trans* retinal values seems unlikely, implying that the assignment of the 1,237 cm^{-1} line as a symmetric combination of the C_{12}—C_{13} and C_{14}—C_{15} stretches is correct.

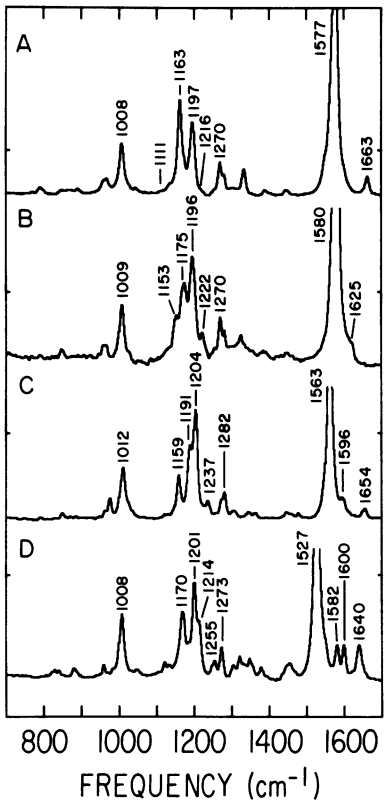

FIGURE 4 Raman spectra of all-*trans* retinal (*A*), its unprotonated Schiff base (*B*), and its PSB (*C*), are compared with the spectrum of BR_{568} (*D*). The retinal and unprotonated Schiff-base spectra were obtained with stationary CCl_4 solutions using 676-nm excitation. The BR_{568} spectrum was obtained with a flowing aqueous suspension of purple membrane using 514.5-nm excitation.

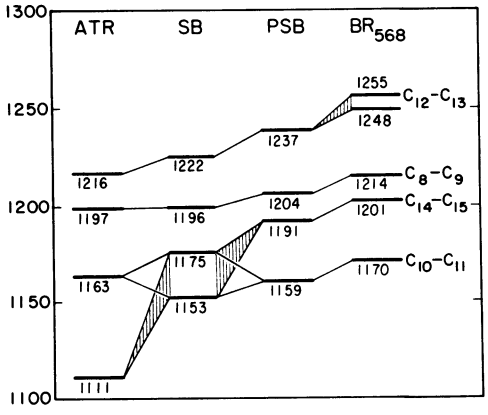

FIGURE 5 Correlation diagram of the C—C single-bond stretches in the fingerprint of all-*trans* retinal (ATR), its Schiff base (SB), its protonated Schiff base (PSB), and BR_{568}. Vibrational levels connected by cross-hatched correlation lines indicate normal modes that are strongly mixed with one another. The additional line that is mixed with the C_{12}—C_{13} stretch at ~1,250 cm^{-1} in BR_{568} may originate from a β-ionone ring or lysine mode (20).

TABLE VI
14,15—di[^{13}C],15D PROTONATED SCHIFF-BASE C—C NORMAL MODES

Frequency		Normal mode
Experimental	Calculated	
cm^{-1}		
1,230	1,221	0.14(12—13) − 0.79(14H) − 0.42(12H)
1,204	1,198	0.15(8—9) − 0.73(10H) − 0.49(12H)
1,190	1,182	0.25(14—15) − 0.36(15D)
—	1,178	0.23(6—7) + 0.40(7H)
1,160	1,162	0.27(10—11) − 0.12(8—9) + 0.32(11H) − 0.02(14—15)

C_8—C_9 and C_{12}—C_{13}, are characteristically higher in frequency at 1,197 and 1,216 cm^{-1}, respectively.

In the Schiff-base spectrum, the frequencies of the 1,196 and 1,222 cm^{-1} lines are very close to the frequencies of the C_8—C_9 and C_{12}—C_{13} stretches in the retinal aldehyde and are therefore reasonably assigned to these modes. Schiff-base formation should affect mainly the vibrations localized near the Schiff-base end of the molecule. The most significant difference observed in the Schiff-base spectrum is the replacement of the 1,163 cm^{-1} C_{10}—C_{11} stretch in the aldehyde by two modes at 1,153 and 1,175 cm^{-1}. ^{13}C-substitution at C_{10} and C_{11} shifts the 1,153 and 1,175 cm^{-1} modes by 9 and 11 cm^{-1}, respectively (Fig. 6 *A*), while ^{13}C-substitution at C_{14} and C_{15} causes a 12 cm^{-1} drop in the 1,175 cm^{-1} line (Fig. 6 *B*). The frequency shift of the 1,153 cm^{-1} line in the 14,15-di[^{13}C] Schiff-base spectrum cannot be determined because of its weak intensity. These shifts argue that the C_{14}—C_{15} stretch has shifted up into near degeneracy with the C_{10}—C_{11} stretch and mixes nearly equally, producing a 20 cm^{-1} splitting between the modes. This picture is supported by 15D substitution,

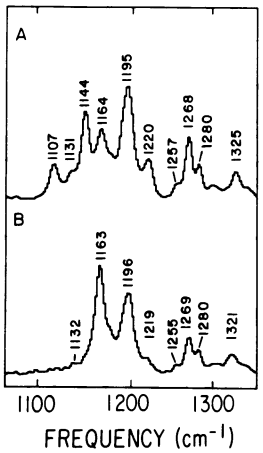

FIGURE 6 Raman spectra of the 10,11-di[^{13}C] (*A*) and 14,15-di[^{13}C] (*B*) unprotonated Schiff bases obtained with stationary CCl_4 solutions using 676-nm excitation.

which shifts the C_{14}—C_{15} component of these mixed modes to higher frequency, leaving the C_{10}—C_{11} stretch near the frequency observed in the aldehyde (1,158 cm^{-1}) (12).

The most interesting question about the Schiff base is the origin of the 1,111 → ~1,163 cm^{-1} frequency increase of the C_{14}—C_{15} stretch. Two possibilities can be identified. First, the Schiff-base nitrogen is less electronegative than the aldehyde oxygen and thus has a weaker attraction for the electrons in nearby bonds. This might cause an increase in the C_{14}—C_{15} bond order and hence an increase in the diagonal force constant. Second, the C_{14}—C_{15} normal mode may be pushed up in frequency as a result of interaction with the new coordinates present in the Schiff base, such as the N—C single bond stretch and the C_{15}=N—C bend. ^{15}N-Substitution does not shift any of the observed fingerprint modes in the Schiff base, suggesting that the N—C stretch is not coupled with the C_{14}—C_{15} stretch. Furthermore, normal mode calculations on the Schiff base show that unless unphysically large coupling constants between the N—C stretch or C_{15}=N—C bend and the C_{14}—C_{15} stretch are used, <15 cm^{-1} of the frequency increase of the C_{14}—C_{15} stretch can be attributed to interaction with these coordinates. We conclude that the dominant factor is an intrinsic increase of the force constant of the C_{14}—C_{15} stretch that presumably results from the reduced electronegativity of the Schiff-base nitrogen.[4]

Protonation of the Schiff-base nitrogen causes an increase in π-electron delocalization, which should be greatest near the Schiff base and decrease toward the ionone ring. The shift in frequencies of the C—C stretches upon protonation is in agreement with this prediction. The frequency increase of the C_{14}—C_{15}, C_{12}—C_{13}, and C_8—C_9 stretches are ~28, 15, and 8 cm^{-1}, respectively. This trend is mirrored in the vibrational calculation which required a 28% increase of K (14–15) and a 14% increase of K (12–13) from the aldehyde values but no significant change in the other C—C stretching constants (Table I). The C_{10}—C_{11} stretch in the PSB drops in frequency ~4 cm^{-1} from its intrinsic, 1,163 cm^{-1} frequency in the Schiff base. This most likely results from coupling of the C_{10}—C_{11} and C_{14}—C_{15} stretches in the PSB as evidenced by the 6 cm^{-1} drop of the 1,191 cm^{-1} C_{14}—C_{15} stretch in the 10,11-di[^{13}C] derivative.

Now that we can trace the changes in the Raman spectrum resulting from Schiff-base formation and protonation, it is interesting to examine the bacteriorhodopsin spectrum to see what effects the protein environment has on the vibrational structure of the retinal chromophore. It

[4]All-valence electron MNDO calculations on acrolein give a reduction in the C_{14}—C_{15} bond length from 1.489 Å in the aldehyde to 1.477 Å in the Schiff base consistent with this picture. Note that QCFF-π calculations were unable to reproduce the increase in the C_{14}—C_{15} stretching frequency in the Schiff base nor was a reduction in bond length predicted.

has been argued that the spectra of BR and its intermediates are difficult to interpret because the protein introduces perturbations that make the pigment spectra very different from the Schiff-base model compounds (12, 15, 28). Comparison of pigment and model compound vibrational assignments allows us to clearly identify both the differences and similarities. Vibrational assignments of the C—C stretches in BR_{568} have recently been made using bacterio-opsin samples regenerated with ^{13}C- and ^{2}H-labeled retinals (Smith, S. O., M. S. Braiman, A. B. Myers, J. A. Pardoen, C. Winkel, P. P. J. Mulder, J. Lugtenburg, and R. Mathies, manuscript in preparation; 29, 30). The C_{14}—C_{15} stretch is assigned at 1,201 cm^{-1}, the C_{10}—C_{11} stretch is at 1,170 cm^{-1}, and the C_8—C_9 stretch is at 1,214 cm^{-1}. As in the PSB the C_{12}—C_{13} stretch in BR_{568} is more delocalized than the other single-bond stretches. C_{12}—C_{13} stretch character is found in the 1,255 cm^{-1} mode as well as a weak line at 1,248 cm^{-1}. There is also significant C_{12}—C_{13} stretch character at 1,170 cm^{-1}. Comparison of the PSB and BR_{568} assignments allows us to conclude that the frequency ordering of the C—C stretches is the same in both molecules, but that all of the C—C stretches are shifted ~10 cm^{-1} higher in frequency by the protein (see Fig. 5). The similar frequency ordering and spacing of the C_8—C_9, C_{10}—C_{11}, C_{12}—C_{13}, and C_{14}—C_{15} stretches suggests that no strong local protein-chromophore perturbations exist in the $C_8 \ldots . C_{15}$ region of the chromophore. This is consistent with the point charge model for BR_{568}, which places a negatively charged amino-acid residue near the ionone ring (31).

The biggest difference between the PSB and BR_{568} is the general upshift of C—C stretches and downshift of C=C stretches. The most obvious explanation is that increased delocalization of the π-system causes an increase in the force constants for the C—C stretches and a decrease in the force constants for the C=C stretches. However, the calculations of Kakitani et al. (32) show that this effect alone is insufficient to explain the observed frequency shifts. An additional possibility is that π-electron delocalization leads to an increase in the potential coupling between the C—C and C=C stretches. Since the potential and kinetic coupling constants between these two basis coordinates have opposite signs, increased delocalization should reduce the net coupling. The effect of reduced C—C, C=C coupling is to increase the frequency of the C—C stretches and decrease the frequency of the C=C stretches, as observed.

Comparison of the isotopic data also allows us to examine the differences between the vibrational properties of the C=N bond in BR_{568} and in the crystalline protonated Schiff base. A detailed analysis of this problem has recently been presented by Kakitani et al. (32) who argued that the low frequency of the 1,640 cm^{-1} Schiff base stretch in BR_{568} was due to reduced coupling with the N—H rock. However, the Schiff-base data available to Katitani et al. exhibited a large range of values for the C=NH stretch frequency (1,650–1,662 cm^{-1}), which makes quantitative interpretation of the differences between the PSB and BR_{568} difficult. Therefore, it is useful to repeat this comparison for crystalline PSB's whose preparation is presumably more reproducible and whose structures can be determined by x-ray or solid-state NMR studies. First, Table IV shows that the ^{15}N- and ^{13}C-induced shifts of the PSB and BR_{568} are very similar. The shifts are 1 to 3 cm^{-1} less in BR_{568}, indicating that the Schiff-base normal mode is only somewhat less localized than in the PSB. To correctly interpret the deuteration-induced shifts we must first assign the C_{15}—H and N—H rocking frequencies. This is because the amount of coupling between the in-plane rocks and the C=N stretch is determined in part by their frequency separation. The C_{15}—H and N—H rocks have been assigned at 1,345 and 1,348 cm^{-1}, respectively, in bacteriorhodopsin (27; Smith, S. O., M. S. Braiman, A. B. Myers, J. A. Pardoen, C. Winkel, P. P. J. Mulder, J. Lugtenburg, and R. Mathies, manuscript in preparation), very close to their assignments in the PSB at 1,345 and ~1,350 cm^{-1}.[5] These frequencies are so similar that we are justified in interpreting any changes in the coupling between the C_{15}—H and N—H rocks and the C=N stretch in terms of altered interaction constants as opposed to altered rock diagonal constants. In the crystalline PSB the ND-induced shift is 23 cm^{-1}, which is 7 cm^{-1} more than that seen in BR_{568}. The 15D-induced shift is 12 cm^{-1}, which is 2 cm^{-1} more than that seen in BR_{568}. Thus the 14 cm^{-1} difference between the frequency of the C=N stretching mode in the crystalline PSB (1,654 cm^{-1}) and in BR_{568} (1,640 cm^{-1}) can be partitioned into 7 cm^{-1} due to reduced N—H rock coupling, 2 cm^{-1} due to reduced C_{15}—H rock coupling, and ~5 cm^{-1} due to a reduction in the intrinsic bond order or indirect interactions. These data indicate that reduced N—H rock to C=N stretch coupling is a significant but by no means the only factor leading to the low C=NH stretch frequency in BR_{568}. Interestingly, the N—H rock coupling in BR_{568} (16 cm^{-1}) is closer to the crystalline PSB (23 cm^{-1}) than the PSBs in solution (25–30 cm^{-1}). This suggests that the crystalline PSBs provide a better model for the hydrogen-bond/counterion environment in BR_{568}.

In summary, the ease with which the C—C stretches in the fingerprint region of the BR_{568} spectrum can be interpreted, once the vibrational assignments of the pigment and the model compound have been determined, illustrates the importance of isotopic derivatives in these studies. A similar analysis of the vibrational spectra of bacteriorhodopsin's 13-*cis* photointermediates should provide additional information about chromophore structure and chromophore-protein interactions that are important

[5]The NH assignment is tentative because a line at this frequency is not clearly resolved in the native PSB spectrum, although intensity is lost between the 1,345 and 1,363 cm^{-1} lines in the ND spectrum.

in proton pumping. Furthermore, the work presented here provides a conceptual framework for analyzing the vibrational structure of the 11-*cis* and 9-*cis* PSB isomers, which are found in the visual pigments, rhodopsin and isorhodopsin.

R. Mathies is a National Institutes of Health Career Development Awardee (EY 00219). S. Smith was supported by a University of California Regents Fellowship and A. Myers was supported by an IBM Fellowship. ^{15}N butylamine was a gift of G. Harbison and R. Griffin.

This research was supported by grants from the National Science Foundation (CHE 8116042) and the National Institutes of Health (NIH (EY-02051). Work carried out in The Netherlands was supported by the Netherlands Foundation for Chemical Research and by the Netherlands Organization for the Advancement of Pure Research.

Received for publication 18 July 1984 and in final form 21 December 1984.

REFERENCES

1. Birge, R. R. 1981. Photophysics of light transduction in rhodopsin and bacteriorhodopsin. *Annu. Rev. Biophys. Bioeng.* 10:315–354.
2. Stoeckenius, W., and R. A. Bogomolni. 1982. Bacteriorhodopsin and related pigments of halobacteria. *Annu. Rev. Biochem.* 51:587–616.
3. Eyring, G., B. Curry, A. Broek, J. Lugtenburg, and R. Mathies. 1982. Assignment and interpretation of hydrogen out-of-plane vibrations in the resonance Raman spectra of rhodopsin and bathorhodopsin. *Biochemistry.* 21:384–393.
4. Mathies, R. 1979. Biological applications of resonance Raman spectroscopy in the visible and ultraviolet: Visual pigments, purple membrane and nucleic acids. *Chem. Biochem. Appl. Lasers.* 4:55–99.
5. Rothschild, K. J., W. A. Cantore, and H. Marrero. 1983. Fourier transform infrared difference spectra of intermediates in rhodopsin bleaching. *Science (Wash. DC).* 219:1333–1335.
6. Bagley, K., G. Dollinger, L. Eisenstein, A. K. Singh, and L. Zimanyi. 1982. Fourier transform infrared difference spectroscopy of bacteriorhodopsin and its photoproducts. *Proc. Natl. Acad. Sci. USA.* 79:4972–4976.
7. Siebert, F., and W. Maentele. 1983. Investigation of the primary photochemistry of bacteriorhodopsin by low temperature Fourier-transform infrared spectroscopy. *Eur. J. Biochem.* 130:565–573.
8. Mathies, R., T. B. Freedman, and L. Stryer. 1977. Resonance Raman studies of the conformation of retinal in rhodopsin and isorhodopsin. *J. Mol. Biol.* 109:367–372.
9. Eyring, G., B. Curry, R. Mathies, R. Fransen, I. Palings, and J. Lugtenburg. 1980. Interpretation of the resonance Raman spectrum of bathorhodopsin based on visual pigment analogues. *Biochemistry.* 19:2410–2418.
10. Doukas, A. G., B. Aton, R. H. Callender, and T. G. Ebrey. 1978. Resonance Raman studies of bovine metarhodopsin I and metarhodopsin II. *Biochemistry.* 17:2430–2435.
11. Aton, B., A. G. Doukas, D. Narva, R. H. Callender, U. Dinur, and B. Honig. 1980. Resonance Raman studies of the primary photochemical event in visual pigments. *Biophys. J.* 29:79–94.
12. Braiman, M., and R. Mathies. 1980. Resonance Raman evidence for an all-*trans* to 13-*cis* isomerization in the proton-pumping cycle of bacteriorhodopsin. *Biochemistry.* 19:5421–5428.
13. Braiman, M., and R. Mathies. 1982. Resonance Raman spectra of bacteriorhodopsin's primary photoproduct: evidence for a distorted 13-cis retinal chromophore. *Proc. Natl. Acad. Sci. USA.* 79:403–407.
14. Marcus, M. A., and A. Lewis. 1978. Resonance Raman spectroscopy of the retinylidene chromophore in bacteriorhodopsin (bR_{570}), bR_{560}, M_{412}, and other intermediates: structural conclusions based on kinetics, analogues, models, and isotopically labeled membranes. *Biochemistry.* 17:4722–4735.
15. Aton, B., A. G. Doukas, R. H. Callender, B. Becher, and T. G. Ebrey. 1977. Resonance Raman studies of the purple membrane. *Biochemistry.* 16:2995–2999.
16. Rimai, L., D. Gill, and J. L. Parsons. 1971. Raman spectra of dilute solutions of some stereoisomers of vitamin A type molecules. *J. Am. Chem. Soc.* 93:1353–1357.
17. Cookingham, R. E., A. Lewis, and A. T. Lemley. 1978. A vibrational analysis of rhodopsin and bacteriorhodopsin chromophore analogues: Resonance Raman and infrared spectroscopy of chemically modified retinals and Schiff bases. *Biochemistry.* 17:4699–4711.
18. Curry, B., A. Broek, J. Lugtenburg, and R. Mathies. 1982. Vibrational analysis of all-trans retinal. *J. Am. Chem. Soc.* 104:5274–5286.
19. Curry, B., I. Palings, A. D. Broek, J. A. Pardoen, P. P. J. Mulder, J. Lugtenburg, and R. Mathies. 1984. Vibrational analysis of 13-*cis* retinal. *J. Phys. Chem.* 88:688–702.
20. Curry, B., I. Palings, A. D. Broek, J. A. Pardoen, J. Lugtenburg, and R. Mathies. 1985. Vibrational analysis of the retinal isomers. *Adv. Infrared Raman Spec.* In press.
21. Saito, S., and M. Tasumi. 1983. Normal coordinate analysis of retinal isomers and assignments of Raman and infrared bands. *J. Raman Spectrosc.* 14:236–245.
22. Lugtenburg, J. 1985. The synthesis of ^{13}C-labelled retinals. *Pure Appl. Chem.* In press.
23. Pardoen, J. A., C. Winkel, P. P. J. Mulder, and J. Lugtenburg. 1984. Synthesis of retinals labelled at positions 14 and 15 (with ^{13}C and/or ^{2}H). *Recl. Trav. Chim. Pays-Bas.* 103:135–141.
24. Pardoen, J. A., H. N. Neijenesch, P. P. J. Mulder, and J. Lugtenburg. 1983. Synthesis of 10-, 11-, 19- and 20-mono-^{13}C-retinal. *Recl. Trav. Chim. Pays-Bas.* 102:341–347.
25. Warshel, A., and M. Karplus. 1974. Calculation of $\pi\pi^*$ excited state conformations and vibronic structure of retinal and related molecules. *J. Am. Chem. Soc.* 96:5677–5689.
26. Oseroff, A. R., and R. H. Callender. 1974. Resonance Raman spectroscopy of rhodopsin in retinal disk membranes. *Biochemistry.* 13:4243–4248.
27. Massig, G., M. Stockburger, W. Gaertner, D. Oesterhelt, and P. Towner. 1982. Structural conclusion on the Schiff base group of retinylidene chromophores in bacteriorhodopsin from characteristic vibrational bands in the resonance Raman spectra of BR_{570} (all-*trans*), BR_{603} (3-dehydroretinal) and BR_{548} (13-*cis*). *J. Raman Spectrosc.* 12:287–294.
28. Terner, J., C.-L. Hsieh, A. R. Burns, and M. A. El-Sayed. 1979. Time-resolved resonance Raman characterization of the $b0_{640}$ intermediate of bacteriorhodopsin. Reprotonation of the Schiff base. *Biochemistry.* 18:3629–3634.
29. Smith, S. O., A. B. Myers, J. A. Pardoen, C. Winkel, P. P. J. Mulder, J. Lugtenburg, and R. Mathies. 1984. Determination of retinal Schiff base configuration in bacteriorhodopsin. *Proc. Natl. Acad. Sci. USA.* 81:2055–2059.
30. Smith, S. O., J. A. Pardoen, P. P. J. Mulder, B. Curry, J. Lugtenburg, and R. Mathies. 1983. Chromophore structure in bacteriorhodopsin's 0_{640} photointermediate. *Biochemistry.* 22:6141–6148.
31. Nakanishi, K., V. Balogh-Nair, M. Arnaboldi, K. Tsujimoto, and B. Honig. 1980. An external point-charge model for bacteriorhodopsin to account for its purple color. *J. Am. Chem. Soc.* 102:7945–7947.
32. Kakitani, H., T. Kakitani, H. Rodman, B. Honig, and R. Callender. 1983. Correlation of vibrational frequencies with absorption maxima in polyenes, rhodopsin, bacteriorhodopsin, and retinal analogues. *J. Phys. Chem.* 87:3620–3628.